ARTICLE

https://doi.org/10.1038/s41586-019-0954-4

A complete catalogue of high-quality topological materials

M. G. Vergniory[1,2,3,11], L. Elcoro[4,11], Claudia Felser[5], Nicolas Regnault[6], B. Andrei Bernevig[7,8,9]* & Zhijun Wang[7,10]*

Using a recently developed formalism called topological quantum chemistry, we perform a high-throughput search of 'high-quality' materials (for which the atomic positions and structure have been measured very accurately) in the Inorganic Crystal Structure Database in order to identify new topological phases. We develop codes to compute all characters of all symmetries of 26,938 stoichiometric materials, and find 3,307 topological insulators, 4,078 topological semimetals and no fragile phases. For these 7,385 materials we provide the electronic band structure, including some electronic properties (bandgap and number of electrons), symmetry indicators, and other topological information. Our results show that more than 27 per cent of all materials in nature are topological. We provide an open-source code that checks the topology of any material and allows other researchers to reproduce our results.

Topological materials have particular topological arrangements in the geometry of their electronic band structures, resulting in robust surface states and unconventional electromagnetic activity. But how many topological materials exist, their identity and their abundance is unclear. The remarkable field of topological insulators and semimetals has combined deep theoretical insights with almost immediate material predictions and their experimental discovery. Since the field began 13 years ago[1–3], the prevalent impression in the physics and chemistry communities has been that topological materials represent an infinitesimal proportion of the total number of materials existing in nature. Even though it has led to a comparatively large number of successes, the method of predicting new topological classes and corresponding materials has so far been based mostly on educated guesses. In this way, time-reversal[2,3], mirror-symmetric and nonsymmorphic topological insulators[4,5]; Dirac[6,7], Weyl[8–11] and nodal-chain[12] semimetals; new fermions[13] and many other states in realistic materials have been predicted. However, the deficiencies of the method are clear: only about 20 topological semimetals have been predicted and experimentally discovered so far. The problem underlying the efficient discovery of materials has been a missing link between the chemistry of different compounds and their topological properties.

In topological quantum chemistry (TQC)[14], a link has been established between the topology of a nonmagnetic material and its crystal symmetry, position and content of the orbitals. The basis of the approach is elementary band representations (EBRs)[15,16], which represent all of the 10,398 (with/without time reversal: 4,757/5,641) building blocks of bands that come from atomic orbitals, and the Brillouin zone compatibility relations[17,18], which provide rules for all of the ways in which electron bands can connect in the Brillouin zone. Both of these features are tabulated on the Bilbao Crystallographic Server (BCS; http://www.cryst.ehu.es), in program BANDREP[19] for EBRs, and program DCOMPREL[20] for the compatibility relations. If a set of valence bands in a material is not a sum of EBRs, then the material is topological[14]; if a set of bands does not satisfy the compatibility relations, then they cannot be separated from others and the material is a semimetal[14,21]. Insulators satisfy the compatibility relations in the Brillouin zone; and if their valence bands cannot be written as a sum of EBRs, then they are topological[14]. An insulator can differ from a sum of EBRs in several ways. The simplest way is that the characters of representations at a certain collection of high-symmetry points called maximal $\boldsymbol{k}$-points cannot be written as a sum of characters of the EBRs in that group (to access the maximal $\boldsymbol{k}$-vectors in the BCS website[19], choose a space group and ask for the elementary band rep (with or without time reversal); the first column gives the maximal $\boldsymbol{k}$-vectors). These are the 'strong' topological phases, which usually exhibit surface or hinge states[22–26]. There are also finer aspects of topology that TQC uniquely captures fully, namely the 'fragile' topological phases, whereby a set of bands can be written as a difference plus a sum (hereafter a 'difference' refers to 'a difference plus a sum') but not purely as a sum of EBRs[15,27–29], with further refinement of topology as in ref. [30]. TQC can so far depict all of the topological phases that exist in nature, at very fine levels of topological refinement. In the original paper[14], TQC was used to predict a set of about 150 new topological materials by targeting groups with a lot of 'disconnected' (or topological) EBRs. We will show how to use TQC to predict new materials in a future publication (Z. Wang et al., manuscript in preparation). Using the EBR data of TQC[14], refs [31,32] obtain a set of strong topological indices that exhaust the strong topological phases[14,33]. These strong indices are equivalent to the EBR equivalence classes defined here.

In this paper, we present a large list of (strong) topological (nonmagnetic) 'high-quality' materials in nature, along with a wide array of information about their structure, bands and topological properties. This work is composed of several research modules, presented in Fig. 1, each of which is essential for finding materials with strong and fragile topology. We outline the steps and results here, and give further details in the Supplementary Information.

Computational approach for finding topological materials

In step A, we wrote a code called VASP2Trace to calculate the characters of all symmetries at all the high-symmetry points of ab initio VASP

[1]Donostia International Physics Center, San Sebastian, Spain. [2]IKERBASQUE, Basque Foundation for Science, Bilbao, Spain. [3]Applied Physics Department II, University of the Basque Country UPV/EHU, Bilbao, Spain. [4]Department of Condensed Matter Physics, University of the Basque Country UPV/EHU, Bilbao, Spain. [5]Max Planck Institute for Chemical Physics of Solids, Dresden, Germany. [6]Laboratoire de Physique de l'École Normale Supérieure, PSL University, CNRS, Sorbonne Université, Université Paris Diderot, Sorbonne Paris Cité, Paris, France. [7]Department of Physics, Princeton University, Princeton, NJ, USA. [8]Physics Department, Freie Universität Berlin, Berlin, Germany. [9]Max Planck Institute of Microstructure Physics, Halle, Germany. [10]Beijing National Laboratory for Condensed Matter Physics, and Institute of Physics, Chinese Academy of Sciences, Beijing, China. [11]These authors contributed equally: M. G. Vergniory, L. Elcoro.
*e-mail: bernevig@princeton.edu; zjwang@princeton.edu

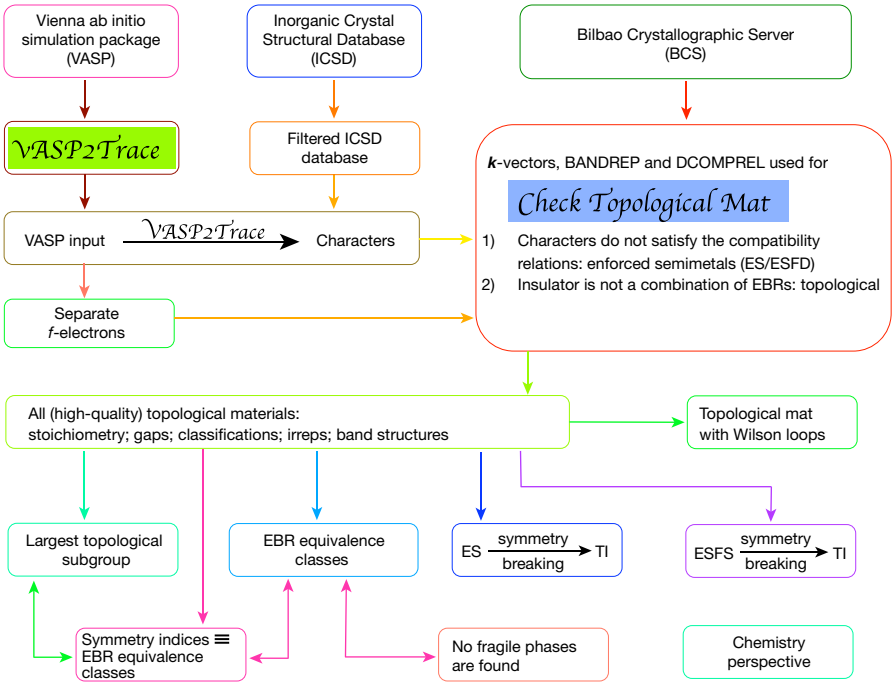

Fig. 1 | Workflow diagram. The figure shows the different codes and calculations used in our search for topological materials. The open-source code VASP2Trace and end-user button CheckTopologicalMat are available online at www.cryst.ehu.es/cryst/checktopologicalmat, and can check the topology of any material. ES, enforced semimetal; TI, topological insulator.

(Vienna ab initio simulation package)[34] wavefunctions. This information did not previously exist for nonsymmorphic symmetries. Details are given in Supplementary Information appendix A, and the code is made available on the BCS[35]. In step B, we scanned the Inorganic Crystal Structure Database (ICSD; http://www2.fiz-karlsruhe.de/icsd_home.html) of 184,270 materials, and removed bad or poor-data compounds by applying the ICSD's 'high-quality' filter (for materials for which the atomic positions and structure are measured very accurately). This filter picked up 89,240 'high-quality' materials, as follows: hexagonal, 16,974; monoclinic-triclinic, 23,355; orthorhombic, 22,430; tetragonal, 13,631; and cubic, 12,850. We then applied the 'stoichiometric', 'few atoms (<30)', 'not alloy' and 'not-usual magnetic atoms' filters to find the total number of stoichiometric compounds: 26,938. We then separated these compounds into 'problematic' *f*-electron compounds (4,286) and 22,652 high-quality stoichiometric, nonproblematic *f*-electron ones. We detail the procedure and the filters in Supplementary Information appendix B.

In step C, we used VASP and the code developed in step A to obtain the characters of all bands at all the relevant high-symmetry points (the maximal ***k***-vectors) for all of the compounds found in step B. The maximal ***k***-vectors are the set of high-symmetry points for which the determination of band characters implies their knowledge everywhere in the Brillouin zone. Details about the set of maximal ***k***-vectors (which can be found by using the BCS[19], as described above), VASP computational parameters, grid mesh and other benchmarks are available in Supplementary Information appendix C. In step D, we wrote a code to check whether a set of characters at the relevant high-symmetry points satisfies the compatibility conditions[17,18] in the Brillouin zone. Furthermore, we wrote another code to check whether—based purely on the characters at high-symmetry points—a set of bands could be expressed as a linear combination of the characters of EBRs, with positive and, crucially, negative coefficients (for finding fragile topology). Self-contained details about these codes, the compatibility relations and our approach are provided in Supplementary Information appendix D.

In step E, we used our codes and the VASP ab initio results to check, for each material, whether the characters obtained in step C satisfy the compatibility relations. If they did not, they are enforced semimetals (the prototypical example being sodium bismuth[7], Na_3Bi). We further separated the enforced semimetals depending on whether they have a high-symmetry point degeneracy at the Fermi level (enforced semimetals with Fermi degeneracy (ESFDs), the prototypical example being bulk mercury telluride, HgTe) or not. If the characters obtained for a given material from step C satisfy the compatibility relations, it means that an insulating filling is possible. We then checked whether the band characters could be written as a sum, or a difference, of the EBRs in the space group. If they could not be written as either a sum or a difference, they are necessarily strong topological. If they could not be written as a sum but could be written as a difference, they are fragile topological[15,27,28]. We then further distinguished the band topology on the basis of whether the band characters could be written as sums of parts of split EBRs[14]. If they could be written as a sum of split (disconnected) EBRs, the materials are denoted SEBRs (the prototypical example being the large spin–orbit coupling (SOC) material graphene). If the band characters could not be written as a sum of split EBRs but were still not a sum or a difference of EBRs, they are denoted more generically 'no linear combination' (NLC) of EBRs (the prototypical compound being calcium arsenide[36], $CaAs_3$).

This partitioning of topological materials into ES, ESFD, SEBR or NLC is based on physical consequences. The ESFDs can become fully insulating when a symmetry-breaking perturbation is applied to the semimetal, and we analyse in step J whether such an insulator is topological or not. In HgTe, upon symmetry breaking, the system becomes a topological insulator. The SEBR insulators are physically similar to graphene: the bands directly below and above the Fermi level, when taken together, form one EBR. In this case, the gap within an EBR has to be topological. The NLC-type materials are physically similar to $CaAs_3$: the bands below and above the Fermi level together form two EBRs, with neither the valence nor the conduction branch being a part of a split EBR. Hence, NLC compounds can be tuned, by slightly varying some parameters, between insulating trivial and insulating nontrivial topological phases; SEBRs can be tuned either to topologically nontrivial insulators or to enforced semimetals. In Supplementary Information appendices D and E, we present the details of our materials classification into the 'physical classes' ES, ESFD, SEBR and NLC. In appendix E, Table I, we present the number of materials, per space group, for each of the classes we define. In Table 1, we provide the

Table 1 | Number of topological materials per space group

SG	TIs	SM	SG	TIs	SM	SG	TIs	SM	SG	TIs	SM	SG	TIs	SM	SG	TIs	SM	SG	TIs	SM
2	101	0	47	13	0	74	25	19	115	5	0	142	0	2	173	0	11	204	24	55
4	0	8	51	17	30	78	0	1	120	0	1	143	0	1	174	0	1	205	6	11
7	0	3	52	0	4	79	0	1	121	9	0	145	0	1	176	2	29	212	0	4
9	0	8	53	2	0	82	8	0	122	15	6	146	0	5	180	0	4	213	0	7
10	1	0	55	63	18	83	1	3	123	55	24	147	2	1	181	0	1	216	8	29
11	98	101	57	9	8	84	1	2	124	0	7	148	54	11	182	0	8	217	7	12
12	390	0	58	12	17	85	1	8	125	5	15	150	0	1	185	0	12	220	4	16
13	13	29	59	33	46	86	0	2	126	0	2	152	0	1	186	0	115	221	14	70
14	71	87	60	7	2	87	11	10	127	37	112	155	0	1	187	0	14	223	0	13
15	95	169	61	2	3	88	0	8	128	1	3	156	0	5	188	0	2	224	0	2
19	0	15	62	257	308	92	0	9	129	177	433	159	0	5	189	44	47	225	30	71
20	0	1	63	223	230	97	0	1	130	0	10	160	0	10	190	2	23	226	0	19
26	0	3	64	26	30	99	0	3	131	2	1	161	0	34	191	20	44	227	88	172
29	0	1	65	57	0	102	0	2	135	0	11	162	5	7	193	8	160	229	1	23
31	0	8	67	1	2	103	0	3	136	14	73	163	2	6	194	57	132	Total	3307	4078
33	0	21	69	18	0	106	0	1	137	3	2	164	102	48	197	0	2			
36	0	15	70	23	5	107	0	4	139	251	99	165	2	3	198	0	34			
40	0	3	71	105	0	109	0	4	140	28	144	166	410	209	199	0	4			
43	0	4	72	9	31	113	4	27	141	24	77	167	92	240	202	0	2			

Shown are the numbers of topological insulators (TIs) and enforced metals or semimetals (SM), at the Fermi level, per space group (SG). Topological insulators consist of both SEBRs and NLCs, while semimetals consist of both enforced semimetals and ESFDs. (See Supplementary Table I for the total number of materials in each class per space group.)

number of 'high-quality' topological insulators or semimetals per space group.

Physical and topological characterization

After finding all the topological materials in our high-quality sample, we moved on to their physical and topological characterization. In step F, we indexed all of the topological materials found in our search by a TQC number (TQC # = SG.*y*.SN#, where SG refers to the space-group number; $y = 1, 2, 3$ or 4 refers to SEBR, NLC, ES or ESFD, respectively; and SN refers to the serial number of the material) for future reference in the entire paper (see Supplementary Table XIV). For each material we provide the following information, in tables. One set of tables (Supplementary Tables XIV–XVI) contains the material's: F1, formula; F2, direct gap; F3, indirect gap; and F4, general class characterization into ES, ESFD, SEBR or NLC. We also provide a set of tables with (F5) all of the representations of the bands below the Fermi level at all of the maximal *k*-points, for each compound; we do this so that the public can perform independent checks. This information is presented in Supplementary Information section F.

In step G, for each of the topological insulating compounds from step E, we provide the symmetry(ies) that stabilizes the compound. Columns 6 and 7 of Supplementary Table XIV list: (1), the minimal topological space subgroup of the compound's space group for which the material is still topological; and (2), the maximal trivial space subgroup of the compound's space group for which the material becomes topologically trivial. Lowering the symmetry of the compound to the space subgroup in (2) renders it trivial; the difference in symmetries between the minimal topological subgroup and the maximal trivial subgroup protects the topological nature of the material.

In step H, for each of the topological insulators from step E, in each space group, we separate the compounds into topological classes: two compounds with band structures related by addition/subtraction of characters of EBRs are equivalent in strong topology. The EBR equivalence classes are identical to the topological indices in refs [31,33]. An equivalent set of indices can be obtained by performing a Smith decomposition on the EBR matrix. We pair up the topological compounds into these classes and provide the information in columns 6 and 7 of Supplementary Table XIV (also in Supplementary Tables XV and XVI, with and without time-reversal symmetry respectively). In Supplementary Information appendices G and H we propose that the topological indices should be understood physically and mathematically as equivalence classes of compounds modulo EBRs, which represents a physical picture of the Smith decomposition of the EBR matrix.

For all enforced semimetals, we provide a different set of relevant information in Supplementary Information appendix I. For the enforced semimetals that we found in step E, we provide the largest subgroup of their space group for which the bands below the Fermi level satisfy the compatibility relations and hence allow an insulating filling. For this insulating filling, we check whether the material is topological by performing the test mentioned in step E for insulators. We then provide the topological classifications of these new insulators obtained by applying symmetry-breaking perturbations to the enforced semimetals.

In step J, for the ESFDs found in step E, we provide the largest subgroup of their space group for which the material satisfies the compatibility relations and allows an insulating filling (Supplementary Table XIX). Given that in ESFDs the degeneracy is at the Fermi level, we have several options for how it splits in the subgroup. The former irreducible representation (irrep) becomes reducible into irreps of the subgroup: one has to choose which irrep moves above or below the Fermi level. The material might also have Fermi degeneracy at other points in the Brillouin zone (for example, related by a symmetry in the group, but not in the lower subgroup), resulting in a mesh of different insulators. For each possibility of an insulating filling, we check whether the material is topological by performing the test in step E for insulators. Supplementary Information appendices I and J give all ways in which semimetals can become topological insulators upon lowering the symmetry. This has practical consequences: this information provides experimentalists with the tools to turn semimetals into topological insulators. Bulk HgTe is an example of this phenomenon: it is an ESFD (with fourfold degeneracy at the Fermi level); however, when its symmetry is broken, a gap opens at the Fermi level to produce a three-dimensional topological insulator.

Computing the electronic band structures

Having enumerated the topological properties of insulating and semimetallic band structures, for all the compounds from step E we obtain

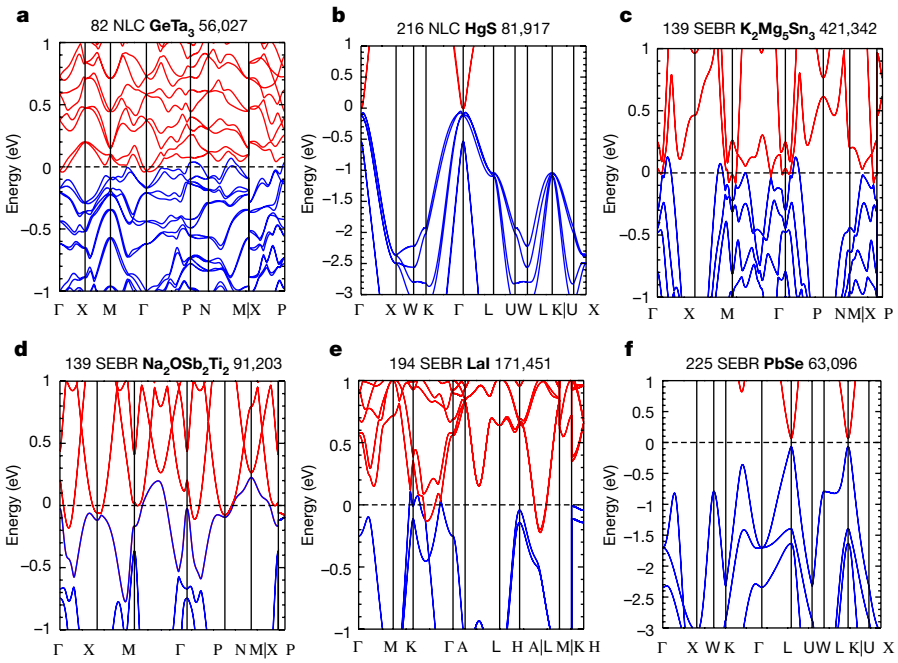

Fig. 2 | Band structures of some newly identified topological compounds. Band structures of $GeTa_3$ (**a**); HgS (**b**); $K_2Mg_5Sn_3$ (**c**); $Na_2OSb_2Ti_2$ (**d**); LaI (**e**) and PbSe (**f**); for all of these compounds, the nontrivial topology is not protected by inversion symmetry. On the *x*-axis are shown relevant points of symmetry in the material's Brillouin zone. At the top of each panel, the first number indicates the space group of the material; the final number indicates the identification code of the material in the ICSD. $GeTa_3$ and HgS are S_4-protected topological insulators, which do not have inversion symmetry. The other materials have inversion symmetry, but their inversion indicators (Z_{2w} and Z_4, as defined in ref. [33]) are zeros (see Supplementary Table IV). In fact, the nontrivial topology is protected by rotational symmetries. Their nontrivial topology is further confirmed by the winding of the Wilson loops (see Supplementary Information appendix L for more details).

and plot the electronic band structure in the Brillouin zone (step K). We provide benchmark parameters for the computation time on the Cobra supercomputer. This task allows for determination of the 'cleanest' topological insulators and semimetals, and is beneficial to experimentalists looking for materials to grow. The band structures are presented in Supplementary Information appendix K.

In step L, for an infinitesimal proportion of some newly identified topological compounds (HgS, $GeTa_3$, $K_2Mg_5Sn_3$, $Na_2OSb_2Ti_2$, LaI and PbSe, the nontrivial topology of which is not protected by inversion symmetry), we perform an in-depth analysis that includes Wilson loops and other holonomy arguments in order to reconfirm the topological nature of the materials. For the first time to our knowledge, we find roto-inversion topological insulator materials in almost all topological classes. We remind the reader of the generic Wilson-loop procedure for obtaining topological invariants in Supplementary Information appendix L. In Fig. 2 we present a very small set of materials; details can be found in appendix L. We also show examples of materials for which the topology is described by all symmetry indicators in Supplementary Table VI, and give their band structures in Supplementary Figs. 8–11.

In Supplementary Information appendix M, for some 4,286 of the compounds that were discarded by our initial filters—such as materials containing 'problematic' *f*-electrons—we present very short tables/summaries, but caution against trusting the ab initio calculations in

Table 2 | Number of materials for different topological indices

Indices	Number of compounds (per space group)
Z_{2w}	87 (2), 61 (11), 298 (12), 9 (13), 42 (14), 37 (15), 10 (47), 13 (51), 1 (53), 38 (55), 5 (57), 21 (59), 122 (63), 21 (64), 47 (65), 1 (67), 15 (69), 73 (71), 6 (72), 21 (74), 1 (83), 1 (84), 7 (87), 27 (123), 5 (125), 26 (127), 117 (129), 1 (131), 122 (139), 13 (140), 1 (147), 32 (148), 2 (162), 63 (164), 215 (166), 10 (191), 13 (204), 9 (221)
Z_4	79 (2), 1 (10), 83 (11), 315 (12), 10 (13), 62 (14), 82 (15), 10 (47), 15 (51), 2 (53), 53 (55), 7 (57), 12 (58), 26 (59), 7 (60), 2 (61), 257 (62), 189 (63), 25 (64), 47 (65), 1 (67), 18 (69), 23 (70), 86 (71), 9 (72), 20 (74), 1 (83), 1 (85), 8 (87), 42 (123), 1 (125), 30 (127), 1 (128), 162 (129), 2 (131), 14 (136), 3 (137), 140 (139), 21 (140), 24 (141), 2 (147), 50 (148), 5 (162), 2 (163), 86 (164), 2 (165), 378 (166), 92 (167), 1 (176), 13 (191), 7 (193), 49 (194), 15 (204), 6 (205), 12 (221), 16 (225), 88 (227), 1 (229)
Z_2	8 (82), 1 (83), 1 (85), 8 (87), 4 (113), 5 (115), 9 (121), 15 (122), 31 (123), 1 (125), 25 (127), 84 (129), 2 (131), 10 (136), 2 (137), 89 (139), 14 (140), 20 (141), 8 (216), 7 (217), 4 (220), 7 (221), 10 (225), 76 (227), 1 (229)
$Z_{4m,pi}$	1 (83), 36 (123), 31 (127), 9 (221)
Z_8	1 (83), 11 (87), 53 (123), 31 (127), 1 (128), 233 (139), 27 (140), 12 (221), 30 (225), 1 (229)
$Z_{3m,0}$	42 (189), 2 (190)
$Z_{3m,pi}$	11 (189)
$Z_{6m,0}$	2 (176), 19 (191), 8 (193), 54 (194)
$Z_{6m,pi}$	16 (191)
Z_{12}	17 (191)
Z_{12}'	2 (176), 8 (193), 57 (194)

Column 1 shows topological indices[32] or EBR equivalence classes (see Supplementary Information appendices H and Q). Column 2 shows the total number of topological compounds (per space group) for an index.

these cases. For step N, we have added a page on the BCS (http://www.cryst.ehu.es/cryst/checktopologicalmat) that enables the user to check whether a material is topological. We provide a short description of all these functionalities in Supplementary Information appendix N.

Our EBR method is uniquely suitable to check for the existence of fragile topological phases, which are undetectable by strong indices. We show in Supplementary Information appendix O that none of the 26,938 materials checked exhibit fragile topology. Next, in step P, we compute several well-known indices of well-known insulators such as topological insulators and higher-order topological insulators, and present the identified compounds in column 10 of Supplementary Table XIV. Alternatively, a topological index is a distinct EBR-equivalent class: two bands are considered in the same class of strong topology if they differ only by a sum or difference of EBRs. This is also computed in step P and is identical to the better known[31,32,37] topological index shown in Supplementary Information appendix Q. In step Q, we compute all of the topological indices[31,32,37] of all bands (satisfying the compatibility relations) and show perfect matching with our EBR equivalence class classification (see appendix Q, with a concise version of this shown in Table 2).

In Supplementary Information appendix R, we provide (for most materials) chemistry-based comments on the difficulty of growing the compound, its air stability, and possible Mott or magnetic tendencies. In Supplementary Information appendix S we provide some 'low-quality' ICSD materials that are topological, and a list of checks performed on both our materials and our topological indices and classification in order to guarantee the accuracy of our data. We have crosschecked some of our compounds with existing literature. Finally, in Supplementary Information appendix T we have compiled a list of about 200 clean/good band structures (for example, a full gap across the Brillouin zone) from our 7,385 topological materials.

Discussion

We have found that roughly 27% of the materials in the world are topological. Roughly 12% are topological insulators. With these findings, we enter an important era of topological material design. One direction will be to compute and discover the physical properties of our large set of materials. Slab calculations should be performed for all of our topological insulators, to reveal their surface states. Compounds for which the topological character is protected by symmetries that are locally preserved by specific surfaces probably exhibit specific states on those surfaces. Compounds for which the topological character is protected by symmetries that are not locally preserved by any specific surface should exhibit hinge states. Rod calculations should be performed for these materials (for example, bismuth[26]). Wilson-loop calculations should be performed for all of the compounds herein. The *d*/*f*-electron compounds that we have predicted should be analysed by more accurate dynamical mean-field theory codes, which properly take into account interactions; these codes can potentially give us many new interacting materials with strong topology. Another step will be to analyse the full ICSD database, and not only the 'high-quality' compounds. Given that we have shown more than one-quarter of all materials to be topological, we are guaranteed to find many others in the ICSD database.

Note added in proof: When finalizing this paper, we became aware of three recent studies that similarly diagnose topological materials[38–40], covering respectively one, five or eight out of the 230 space groups in their searches.

Data availability

All data is available in the Supplementary Information.

Online content

Any methods, additional references, Nature Research reporting summaries, source data, statements of data availability and associated accession codes are available at https://doi.org/10.1038/s41586-019-0954-4.

Received: 5 July 2018; Accepted: 27 December 2018;
Published online 27 February 2019.

1. Kane, C. L. & Mele, E. J. Quantum spin Hall effect in graphene. *Phys. Rev. Lett.* **95**, 226801 (2005).
2. Bernevig, B. A., Hughes, T. L. & Zhang, S.-C. Quantum spin Hall effect and topological phase transition in HgTe quantum wells. *Science* **314**, 1757–1761 (2006).
3. Fu, L. & Kane, C. L. Topological insulators with inversion symmetry. *Phys. Rev. B* **76**, 045302 (2007).
4. Wang, Z., Alexandradinata, A., Cava, R. J. & Bernevig, B. A. Hourglass fermions. *Nature* **532**, 189–194 (2016).
5. Wieder, B. J. et al. Wallpaper fermions and the nonsymmorphic Dirac insulator. *Science* **361**, 246–251 (2018).
6. Wang, Z., Weng, H., Wu, Q., Dai, X. & Fang, Z. Three-dimensional Dirac semimetal and quantum transport in Cd_3As_2. *Phys. Rev. B* **88**, 125427 (2013).
7. Wang, Z. et al. Dirac semimetal and topological phase transitions in A_3Bi (A = Na, K, Rb). *Phys. Rev. B* **85**, 195320 (2012).
8. Weng, H., Fang, C., Fang, Z., Bernevig, B. A. & Dai, X. Weyl semimetal phase in non- centrosymmetric transition-metal monophosphides. *Phys. Rev. X* **5**, 011029 (2015).
9. Huang, S.-M. et al. An inversion breaking Weyl semimetal state in the TaAs material class. *Nat. Commun.* **6**, 7373 (2015).
10. Lv, B. Q. et al. Experimental discovery of weyl semimetal TaAs. *Phys. Rev. X* **5**, 031013 (2015).
11. Xu, S.-Y. et al. Discovery of a weyl fermion semimetal and topological Fermi arcs. *Science* **349**, 613–617 (2015).
12. Bzdušek, T., Wu, Q., Rüegg, A., Sigrist, M. & Soluyanov, A. Nodal-chain metals. *Nature* **538**, 75–78 (2016).
13. Bradlyn, B. et al. Beyond Dirac and Weyl fermions: unconventional quasiparticles in conventional crystals. *Science* **353**, aaf5037 (2016).
14. Bradlyn, B. et al. Topological quantum chemistry. *Nature* **547**, 298–305 (2017).
15. Cano, J. et al. Topology of disconnected elementary band representations. *Phys. Rev. Lett.* **120**, 266401 (2018).
16. Elcoro, L. et al. Double crystallographic groups and their representations on the Bilbao Crystallographic Server. *J. Appl. Crystallogr.* **50**, 457–1477 (2017).
17. Vergniory, M. G. et al. Graph theory data for topological quantum chemistry. *Phys. Rev. E* **96**, 023310 (2017).
18. Bradlyn, B. et al. Band connectivity for topological quantum chemistry: band structures as a graph theory problem. *Phys. Rev. B* **97**, 035138 (2018).
19. Band representations of the double space group (BANDREP). *Bilbao Crystallographic Server* www.cryst.ehu.es/cryst/bandrep.
20. Compatibility relations between representations of the double space groups (DCOMPREL). *Bilbao Crystallographic Server* www.cryst.ehu.es/cryst/dcomprel.
21. Kruthoff, J., de Boer, J., van Wezel, J., Kane, C. L. & Slager, R.-J. Topological classification of crystalline insulators through band structure combinatorics. *Phys. Rev. X* **7**, 041069 (2017).
22. Benalcazar, W. A., Bernevig, B. A. & Hughes, T. L. Quantized electric multipole insulators. *Science* **357**, 61–66 (2017).
23. Schindler, F. et al. Higher-order topological insulators. *Sci. Adv.* **4**, eaat0346 (2018).
24. Song, Z., Fang, Z. & Fang, C. (d−2)-dimensional edge states of rotation symmetry protected topological states. *Phys. Rev. Lett.* **119**, 246402 (2017).
25. Langbehn, J., Peng, Y., Trifunovic, L., von Oppen, F. & Brouwer, P. W. Reflection-symmetric second-order topological insulators and superconductors. *Phys. Rev. Lett.* **119**, 246401 (2017).
26. Schindler, F. et al. Higher-order topology in bismuth. *Nat. Phys.* **14**, 918–924 (2018); correction **14**, 1067 (2018).
27. Po, H. C., Watanabe, H. & Vishwanath, A. Fragile topology and wannier obstructions. *Phys. Rev. Lett.* **121**, 126402 (2017).
28. Bouhon, A., Black-Schaffer, A. M. & Slager, R.-J. Wilson loop approach to topological crystalline insulators with time reversal symmetry. Preprint at https://arxiv.org/abs/1804.09719 (2018).
29. Song, Z. et al. All "magic angles" are "stable" topological. Preprint at https://arxiv.org/abs/1807.10676 (2018).
30. Bradlyn, B., Wang, Z., Cano, J. & Bernevig, B. A. Disconnected elementary band representations, fragile topology, and Wilson loops as topological indices. *Phys. Rev. B* **99**, 045140 (2019).
31. Song, Z., Zhang, T., Fang, Z. & Fang, C. Quantitative mappings between symmetry and topology in solids. *Nat. Commun.* **8**, 3530 (2018).
32. Song, Z., Zhang, T. & Fang, C. Diagnosis for nonmagnetic topological semimetals in the absence of spin-orbital coupling. *Phys. Rev. X* **8**, 031069 (2018).
33. Po, H. C., Vishwanath, A. & Watanabe, H. Symmetry-based indicators of band topology in the 230 space groups. *Nat. Commun.* **8**, 50 (2017).
34. Kresse, G. & Hafner, J. Ab initio molecular dynamics for liquid metals. *Phys. Rev. B* **47**, 558–561 (1993).
35. Check Topological Mat. *Bilbao Crystallographic Server* www.cryst.ehu.es/cryst/checktopologicalmat.
36. Xu, Q., Yu, R., Fang, Z., Dai, X. & Weng, H. Topological nodal line semimetals in the CaP_3 family of materials. *Phys. Rev. B* **95**, 045136 (2017).
37. Fang, C. & Fu, L. Rotation anomaly and topological crystalline insulators. Preprint at https://arxiv.org/abs/1709.01929 (2017).
38. Zhou, X. et al. Topological crystalline insulator states in the Ca_2As family. *Phys. Rev. B* **98**, 241104(R) (2018).
39. Tang, F., Po, H. C., Vishwanath, A. & Wan, X. Efficient topological materials discovery using symmetry indicators. Preprint at https://arxiv.org/abs/1805.07314 (2018).

40. Tang, F., Po, H. C., Vishwanath, A. & Wan, X. Topological materials discovery by large-order symmetry indicators. Preprint at https://arxiv.org/abs/1806.04128 (2018).

Acknowledgements We thank B. Bradlyn, J. Cano and M. Aroyo for countless discussions and collaborations, and for their help with the development of the BANDREP section of the BCS, without which none of the present work would have been possible. We thank H. Gross, S. Parkin, U. Schmidt, M. Rampp and the computational resources of the Max Planck Institute at Halle and Garching, as well as the staff at the Atlas supercomputer of the Donostia International Physics Center. We are grateful to H. Lederer and I. Weidl for allowing us access to the Cobra Supercomputer at the Max Planck Gesellschaft (MPG) computing centre. We also thank H. Borrmann of the Max Planck Institute in Dresden for help with the ICSD database. L.E. was supported by the Government of the Basque Country (project IT779-13), the Spanish Ministry of Economy and Competitiveness (MINECO), and the European Fund for Economic and Regional Development (FEDER; project MAT2015-66441-P). M.G.V. was supported by national project IS2016-75862-P of the Spanish MINECO. B.A.B. and Z.W. acknowledge support for the analytical work from the Department of Energy (de-sc0016239), a Simons Investigator Award, the Packard Foundation, and the Schmidt Fund for Innovative Research. Z.W. was also supported by the CAS Pioneer Hundred Talents Program. The computational part of the Princeton work was performed under National Science Foundation (NSF) Early-concept Grants for Exploratory Research (EAGER): DMR 1643312 NOA-AWD1004957, ONR-N00014-14-1-0330, ARO MURI W911NF-12-1-0461, NSF-MRSECDMR-1420541.

Reviewer information *Nature* thanks Joseph Checkelsky, Marcel Franz and the other anonymous reviewer(s) for their contribution to the peer review of this work.

Author contributions All authors contributed to performing the calculations and analysing the results.

Competing interests The authors declare no competing interests.

Additional information
Supplementary information is available for this paper at https://doi.org/10.1038/s41586-019-0954-4.
Reprints and permissions information is available at http://www.nature.com/reprints.
Correspondence and requests for materials should be addressed to B.A.B. or Z.W.
Publisher's note: Springer Nature remains neutral with regard to jurisdictional claims in published maps and institutional affiliations.